LEGIBILITY NOTICE

A major purpose of the Technical Information Center is to provide the broadest dissemination possible of information contained in DOE's Research and Development Reports to business, industry, the academic community, and federal, state and local governments.

Although a small portion of this report is not reproducible, it is being made available to expedite the availability of information on the research discussed herein.

Los Alamos National Laboratory is operated by the University of California for the United States Department of Energy under contract W-7405-ENG-36

LA-UR--87-3149

DE88 000496

TITLE SYNTHESIS OF MONOCLINIC YTTRIA BY THERMAL PLASMA PROCESSING

AUTHOR(S) Gerald J. Vogt
Materials Technology: Metallurgy and Ceramics
Materials Science and Technology Division

SUBMITTED TO 172nd Meeting of The Electrochemical Society, Inc.
Honolulu, Hawaii
October 18-23,1987

DISCLAIMER

MASTER

Los Alamos Los Alamos National Laboratory
Los Alamos, New Mexico 87545

SYNTHESIS OF THE MONOCLINIC YTTRIA BY THERMAL PLASMA PROCESSING

Gerald J. Vogt

Materials Science and Technology Division
Los Alamos National Laboratory
Los Alamos, New Mexico 87545

ABSTRACT

Submicron powders of monoclinic yttria were prepared by thermal plasma processing of commercial yttria powder. The starting yttria powder was vaporized in the hot tail flame of a thermal argon plasma and the resulting vapor was quenched with hydrogen gas to form yttria particles with a 21-nm mean diameter. The synthesis of yttria by oxidizing yttrium carbide in the plasma was also examined. The plasma powders were characterized by powder x-ray diffraction, transmission electron microscopy, and differential thermal analysis.

INTRODUCTION

The common crystal structure of yttria is cubic with the space group Ia3, a = 1.0604 nm [1]. Like the rare earth sesquioxides, yttria can exhibit polymorphism, existing in a metastable monoclinic phase after high pressure synthesis [2] or upon rapid solidification processing [3-4]. For the rare earth sesquioxides, lanthanum, cerium, and praseodymium with the largest ionic radii exist as a hexagonal A form, whereas elements samarium to dysprosium with smaller ionic radii exhibit the cubic C form at lower temperatures and the monoclinic B form at higher temperatures. The oxides of elements holmium to lutetium, plus yttrium, with the smallest ionic radii commonly exhibit only the cubic C form.

Yttria is known to retain the C form for temperatures up to 2030 K [5], although Hoekstra and Gingerich [6] speculated early that yttria may transform to the B form at temperatures near its melting point (≈2710 K) [7]. The high temperature studies by Foex and Traverse [8], however, failed to find any evidence for a B yttria phase between 2000 K and the melting point of yttria. Interestingly, a hexagonal phase was observed above 2520 K and characterized by x-ray diffraction at 2600 K.

Rapid quenching of molten materials can often lead to retention of a high temperature crystal phase at lower temperatures by rapidly cooling microparticles without a phase transformation occurring. This phenomenon is commonly observed in thermal plasma processing or synthesis [4,9-12], where quenching rates of the process gas can range from 10^3 to 10^8 K/s. For example, metastable phases (e.g., gamma,

delta, and theta phases of alumina) and metastable high temperature phases (e.g., tetragonal phases of zirconia and hafnia) have been observed by the rapid quenching of submicron particles. In this work, plasma processing was used to prepare submicron Y_2O_3 particles of either the B or C structure. The crystal structure and lattice constants for the plasma powders were investigated by powder x-ray diffraction. The thermal stability of monoclinic yttria and the B-to-C transition temperature range were examined by differential thermal analysis and by static annealing tests in air.

EXPERIMENTAL

Plasma yttria was prepared from commercially available starting powder of yttria and yttrium carbide. The starting Y_2O_3 was a -325 mesh powder of a 99.9% purity. The starting powder was further characterized at our laboratory, giving a BET surface area of 0.52 m^2/g and a median particle size of 23 microns with an Elzone Particle Sizer. The YC_2 powder was 99% pure, relative to rare earth metals, at a -325 mesh. These coarse powders were transported with an Ar/O_2 carrier gas and axially injected into the tail flame of a thermal argon plasma [9,11,12], shown in Figure 1. The starting powders were injected into the plasma gas at an axial point level with the lowest turn of the primary rf-coil. The starting powder feed rates and carrier gas compositions are summarized in Table 1 with the synthesis results.

The submicron powders were prepared in a plasma reactor, shown in Figure 1, utilizing an inductively-coupled plasma as described earlier [9,11,12]. The plasma operating conditions are given in Table 2. After vaporizing the starting powder in the hot tail flame, the submicron powders nucleated and grew in the argon process gas rapidly quenched with a room-temperature argon/hydrogen gas stream. The quenching gas was injected using the radial injector scheme, shown in Figure 1b, with four orthogonal 3-mm jets positioned 18 cm below the injection point of the reactants. The radial quenching design was used in these experiments because it provided more efficient gas quenching than the annular design. The reactor in Figure 1 was mounted vertically with the process gas flowing in the direction of gravity and was equipped with a trap at the bottom to collect non-vaporized particles. The submicron particles after exiting the reactor were collected on metallic filters downstream of the reactor and then handled in laboratory air.

The crystal structure of the plasma-produced powders was determined by x-ray diffraction (XRD) with a Scintag PAD V diffractometer using CuKα radiation with a graphite monochromator. Lattice constants were determined from samples containing an internal 2-theta standard of either silver or silicon powder. A least-squares cell refinement program [13] was used to index the XRD patterns and to refine the lattice constants. The powder morphology was examined by transmission electron microscopy. Specific BET surface areas were measured by the multipoint method. The B-to-C transformation was

examined by differential thermal analysis with a heating rate of 10°C/min in a flowing argon atmosphere.

RESULTS AND DISCUSSION

The synthesis results and physical properties of the plasma powders taken from the powder collector are given in Table 1. The white yttria powder samples prepared from starting Y_2O_3 had large surface areas greater than 50 m^2/g; whereas, the plasma yttria from starting YC_2 had a surface area near 20 m^2/g. The surface areas for powders 1, 2, and 3 correspond to a mean equivalent spherical diameters of 20, 21, and 56 nm, using a theoretical density of 5.47 g/cm^3 for B form yttria. The smaller particle sizes obtained from starting Y_2O_3 compared to those from YC_2 are probably the result of less particle growth from the yttrium vapor phase due to smaller partial pressures of yttrium-oxygen species produced by vaporizing yttria.

A single density determination for powder 3 yielded an experimental density of 4.98 g/cm^3, which is 91.0% of the theoretical density for monoclinic yttria. The measurement was done with an automatic pycnometer with a helium working gas. The low result is probably due to the presence of adsorbed water on the fine particles, as the sample was not heated to remove adsorbed gases and vapors.

Transmission electron micrographs of the plasma yttria indicate a generally spheroidal particle shape with some faceting, as seen in Figure 2. The yttria powders appeared to be loosely agglomerated single particles with little hard agglomeration, as evident by lack of bridging or wetting at the interparticle contact points. In Figure 2a the particle diameters for powder 2 range from 10 to 100 nm with the majority of particles between 10 and 50 nm. This observed size range qualitatively agrees with the BET surface area measurements.

The yield of submicron monoclinic Y_2O_3 from coarser yttria was typically 3 to 4% of the amount of starting powder injected. Mass balance of the powders within the reactor showed that approximately 25% of the Y_2O_3 powder was deposited on the water-cooled reactor wall and approximately 70% was found in plumbing and powder trap at the bottom of the reactor. Measured BET surface areas for these two fractions were generally 20 and <1.0 m^2/g, respectively. This observation suggested that perhaps less than 25% of the injected Y_2O_3 was vaporized and recondensed in the argon plasma of the reactor. In order to increase the yield of submicron monoclinic Y_2O_3, a nitrogen or hydrogen/argon plasma with its far greater gas enthalpy would be desirable to vaporize a larger fraction of the injected yttria. However, in this work an alternate synthesis reaction was investigated for the argon plasma by preparing submicron yttria from a starting yttrium carbide powder reacted with excess molecular oxygen.

Powder 3 in Table 1 was prepared by the plasma oxidation of yttrium carbide. In experiment 3 oxygen level in the carrier gas was approximately 120-times greater than stoichiometric for yttria. As a result, the conversion of carbide to oxide was essentially complete for this reactive carbide. The yield of submicron yttria at the filter collector increased by ten-fold to 31%. However, as a necessary trade-off for a greater yield of oxide, the starting carbide, as expected, was far more difficult to feed at a nearly constant feed rate than the starting commercial yttria.

The powders collected on the filters consisted largely of the monoclinic B form of yttria with minor amounts of the C form, as seen from the XRD patterns in Figure 3. In the XRD patterns, the cubic C form was present primarily as a <222> shoulder peak on the monoclinic <111> peak. The plasma yttria prepared from YC_2 had a larger fraction of cubic yttria, as evident in Figure 3. Figure 4 illustrates the typical powder x-ray diffraction pattern for powder 2 over the 2-theta range from 25° to 65°. The $CuK\alpha_1$ peak positions agreed quite well with those values derived from the previously reported crystallographic constants [2-3].

The measured lattice constants for monoclinic yttria, space group C2/m, are given in Table 3 with the earlier values of Hoekstra [2] and Coutures et al. [3]. The indexed powder diffraction pattern for powder 3 is given in Table 4 with the observed and fitted d-values. The lattice constants for powders 2 and 3 are quite consistent with each other and with the earlier values of Hoekstra [2] and Coutures et al. [3]. Using the value for the cell volume of powder 3, the theoretical density of monoclinic Y_2O_3 was calculated to be 5.47 g/cm^3 for Z = 6 [2], which is 8.7% greater than the theoretical density of cubic yttria (5.03 g/cm^3) [1].

There are some small, but significant, differences among the fitted values for the lattice constants, especially for the a constants. The values for constant a in powders 2 and 3 differ by 0.025 angstrom, where the constant a for powder 2 is approximately 0.18% larger than the a value for powder 3. This difference appears to be significant, perhaps representing a quenching or other processing effect during particle growth from a yttria starting powder. Coutures et al. [3] observed a larger processing effect on constant c in their study of the rapid solidification of yttria vapor onto a cold substrate. As seen in Table 3, the value of constant c was larger by 0.30 angstrom (3.6%) when the yttria was condensed in a hydrogen atmosphere, rather than in a nitrogen atmosphere. They also observed in their XRD work that the condensates obtained under nitrogen were better crystallized than those obtained under hydrogen. Similarly, in this work plasma powders prepared from the carbide appeared to be better crystallized than those prepared from the oxide. However, the line broadening found in the XRD patterns for powders 1 and 2 was definitely attributable to a particle size effect as indicated by the large BET surface areas given in Table 1.

The thermal stability of monoclinic yttria was examined by DTA measurements in a flowing argon atmosphere. For a heating rate of 10°C/min, powders 2 and 3 underwent a transformation to cubic C yttria with the onset at approximately 1300 ± 25 K and ending by 1400 K; the maximum exothermic release of heat was at approximately 1330 ± 25 K. DTA measurements of the enthalpy of transformation for powder 2 varied from -3 to -9.3 kJ/mole, although the actual value is believed to be between -6 and -9 kJ/mole. The cause for the widely varying DTA values for the transition enthalpy is not known at this time, pending further study. From his high-pressure data, Hoekstra [2] estimated an enthalpy change of approximately +8 kJ/mole for the C-to-B transformation. The complete conversion of the B form to the C form in the DTA samples was confirmed by powder x-ray diffraction.

Monoclinic yttria will slowly transform to cubic yttria when heated in air at temperatures just below 1300 K for a duration of greater than one hour. Hoekstra [2] reported that cubic yttria will appear after annealing in air at 1173 K (900°C) for several hours. Similarly, in this work powder 2 slowly transformed to cubic yttria at 1173 K upon annealing in air. Heating for one hour gave measurable changes in the relative peak intensities in the powder XRD pattern. The thermal conversion rate at 1173 K was quite slow with a significant fraction of monoclinic yttria still present after ten hours of heating.

CONCLUSIONS

The submicron yttria particles were readily prepared by axially injecting yttria and yttrium carbide with oxygen into a thermal rf-plasma tail flame. The major crystalline phase of these powders was the metastable monoclinic B form commonly observed in rare earth sesquioxides. The monoclinic B form rapidly transformed to the common cubic C form after several minutes at temperatures above 1300 K and quite slowly, taking many hours, at temperatures below 1300 K. The enthalpy for the B-to-C transformation was estimated to be less than -9.3 kJ/mole, although a precise value could not be determined by DTA measurements.

ACKNOWLEDGMENTS

The author wishes to thank the Institutional Supporting Research and Development program of the Los Alamos National Laboratory and the Sandia National Laboratory, Albuquerque, for supporting this work. Also, the author expresses his gratitude to Dr. R. Schwarz and Dr. E. Foltyn for their DTA measurements of the plasma synthesized yttria.

REFERENCES

1. Powder Diffraction File Card 25-1200, Joint Committee on Powder Diffraction Standards, Swarthmore, Pa.
2. H.R. Hoekstra, J. Inorg. Chem. 5, 754 (1966).
3. J.P Coutures, J. Coutures, R. Renard, and G. Benezech, Comp. Rend. Acad. Sci., Ser. C, 275, 1203 (1972).
4. R. McPherson, J. Mater. Sci. 18, 1341 (1983).
5. K. Hirata, K. Moriya, and Y. Waseda, J. Mater. Sci. 12, 838 (1977).
6. H.R. Hoekstra and K.A Gingerich, Science 145, 1164 (1964).
7. F. Cabannes, V.T. Loc, J.P. Coutures, and M. Foex, High Temp.-High Press. 8, 391 (1976).
8. M. Foex and J.P. Traverse, Rev. Int. Hautes Temper. et Refract. 3, 429 (1966).
9. G.J Vogt and L.R. Newkirk, "Thermal Plasma Chemical Synthesis of Powders," Proceedings of the Symposium on High Temperature Materials Chemistry-III, (The Electrochemical Society, Inc., Pennington, NJ), 164 (1986).
10. R. McPherson, J. Mater. Sci. 8, 851 (1973).
11. G.J. Vogt, D.S. Phillips, and T.N. Taylor, "Plasma Synthesis and Characterization of Ultrafine SiC," in Advances in Ceramics, Vol. 21, Ceramic Powder Science, G.L Messing et al. eds., (American Ceramic Society, Westerville, Ohio, 1987) pp. 203-215.
12. G.J. Vogt, R. Vigil, L. Newkirk, and M. Trkula, "Synthesis of Ultrafine Ceramic and Metallic Powders in a Thermal Argon RF-Plasma," Seventh International Symposium on Plasma Chemistry, Eindhoven, 668 (1985).
13. D. Appleman and H. Evans, Jr., Report #PB216188 (1973), U.S. Dept. of Commerce, National Technical Information Service, 5285 Port Royal Rd., Springfield, VA.

Table 1. Synthesis Results For Powders Collected On Filters.

Experiment No.	1	2	3
Carrier Ar (slpm)	4.1	4.1	3.8
Carrier O_2 (slpm)	0.025	0.050	2.9
Mean Feed Rate (g/min)	0.56	0.67	0.16
Per Cent Yield[a]	3.5	3.2	31
BET Surface Area (m^2/g)	55.4	52.9	19.6

[a] Yield at filter collector relative to the theoretical yield.

Table 2. Plasma Operating Conditions

Experiment No.	1	2	3
Plate Power (kW)	37	39	41
Frequency (kHz)	360	357	363
Plasma Ar (slpm)	30	31	31
Quench Ar (slpm)	6.0	5.8	6.5
Quench H_2 (slpm)	6.1	6.1	6.1

Table 3. Lattice Constants for Monoclinic Yttria.

Reference	a (A)	b (A)	c (A)	Beta (degree)	cell volume (A^3)
Hoekstra (2)	13.91	3.483	8.593	100.15	409.80
Coutures (3) (in H_2)	13.90	3.489	8.901	100.06	425.04
(in N_2)	13.90	3.485	8.598	100.11	410.03
Powder #2[a]	13.9245	3.4900	8.6127	100.20	411.94
	0.0041	0.0009	0.0031	0.03	0.16
Powder #3[a]	13.8992	3.4934	8.6118	100.27	411.44
	0.0024	0.0005	0.0013	0.02	0.08

[a]Estimated uncertainty from the least-squares fit are given below the value for the lattice constants.

Table 4. Powder Diffraction Data for Monoclinic Yttria Powder 3 with the Fitted d-values[a].

d(obs) (A)	I/Io (%)	h	k	l	d(calc) (A)
5.858	4	2	0	-1	5.866
3.930	7	2	0	-2	3.929
3.346	20	2	0	2	3.344
3.097	95	1	1	1	3.096
2.992	83	4	0	1	2.991
2.929	96	4	0	-2	2.928
2.824	43	0	0	3	2.825
2.774	75	3	1	0	2.773
2.704	100	1	1	-2	2.703
2.589	4	1	1	2	2.589
2.280	18	6	0	0	2.279
2.217	9	1	1	-3	2.217
2.162	21	5	1	-1	2.161
2.120	8	0	0	4	2.118
2.095	61	3	1	-3	2.096
1.879	75	3	1	3	1.879
1.819	4	5	1	2	1.819
1.760	7	1	1	4	1.761
1.747	38	0	2	0	1.747
1.674	47	7	1	-2	1.675
1.625	34	7	1	1	1.624
1.543	14	1	1	-5	1.543
1.508	21	4	2	1	1.508
1.500	25	4	2	-2	1.500
1.486	12	0	2	3	1.486
1.464	8	8	0	-4	1.464

[a] The fitted d-values were calculated from the lattice constants given in Table 3.

Figure Captions.

Figure 1a. Schematic of inductively-coupled plasma reactor used to prepare submicron yttria powders.

Figure 1b. Schematic of annular and radial quench gas injection systems. Both quenching designs can be used with the plasma reactor.

Figure 2. Microstructure of plasma synthesized yttria powder. Particles were prepared from (a) micron-sized Y_2O_3 powder and from (b) coarse YC_2 powder. The particles appear to be single crystals of roughly spherical shape.

Figure 3. XRD patterns over a 25-35° 2-theta range for (a) powder 1 and (b) powder 3, showing the most characteristic reflections for monoclinic B yttria. The two peaks labelled with a "C" correspond to the <222> and <400> reflections for the cubic C phase.

Figure 4. Typical XRD powder pattern for powder 2 over a 25-65° 2-theta range.

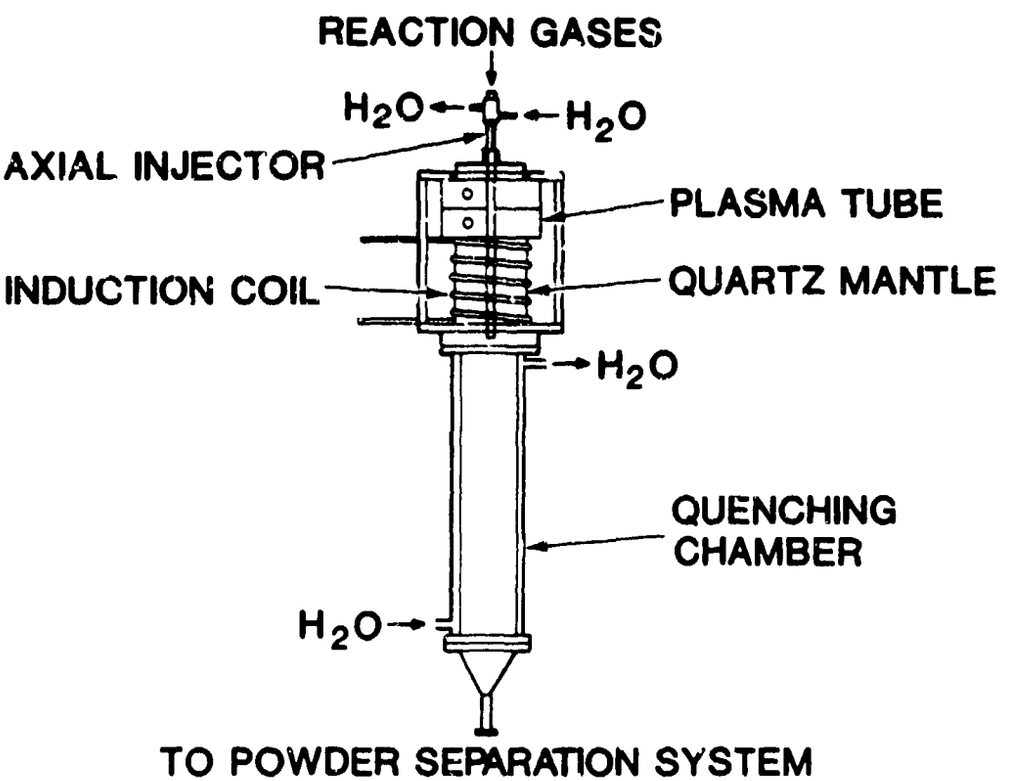
REACTION GASES
H_2O
H_2O
AXIAL INJECTOR
PLASMA TUBE
INDUCTION COIL
QUARTZ MANTLE
H_2O
QUENCHING CHAMBER
H_2O
TO POWDER SEPARATION SYSTEM

Fig 1a

Fig 16

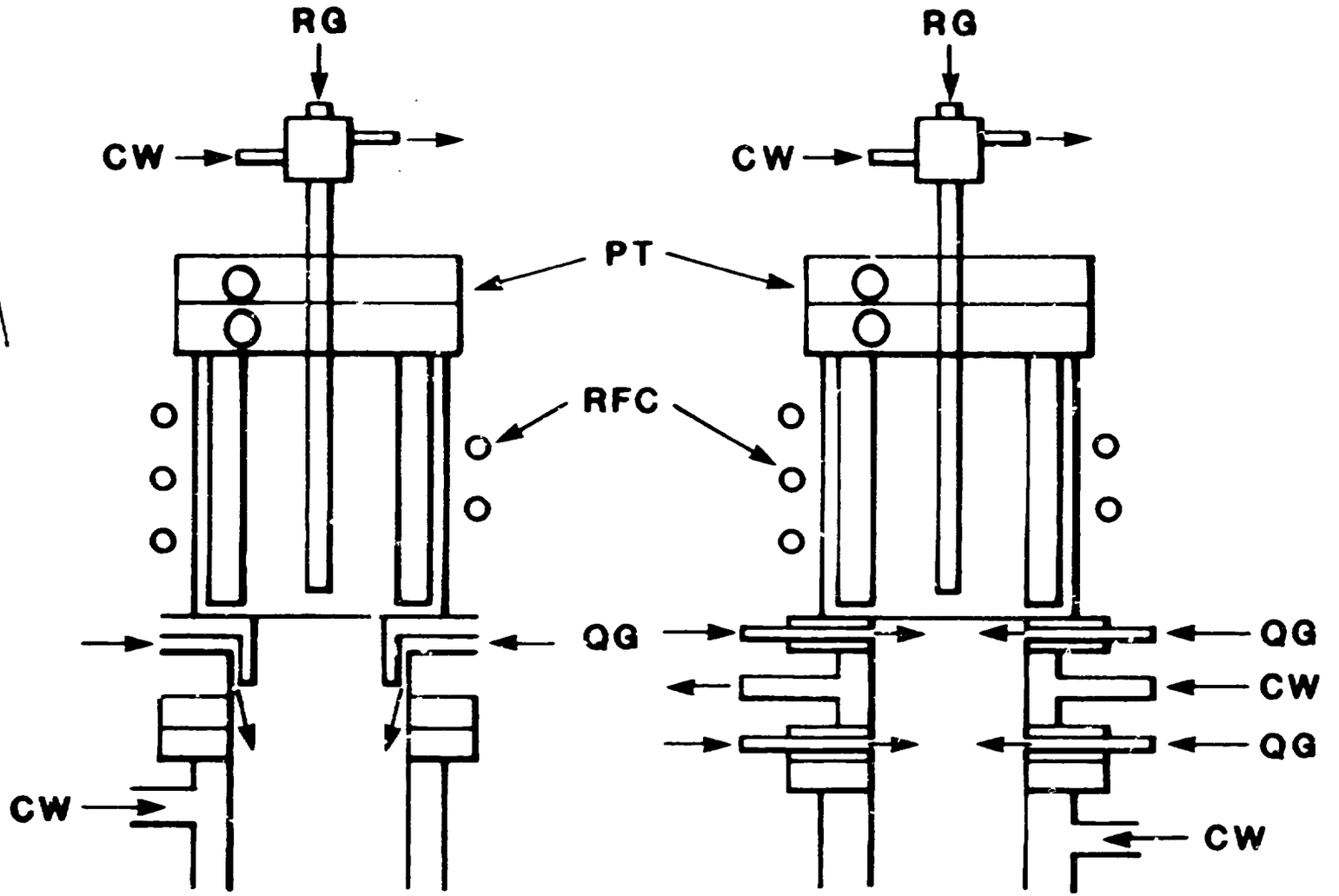

ANNULAR

RADIAL

PT - PLASMA TUBE

RG - REACTANTS

QC - QUENCH GAS

CW - COOLING WATER

RFC - RF COIL


100000 X


SWLA 2000FX
001247 200.0KV X20K 200nm

Fig 3

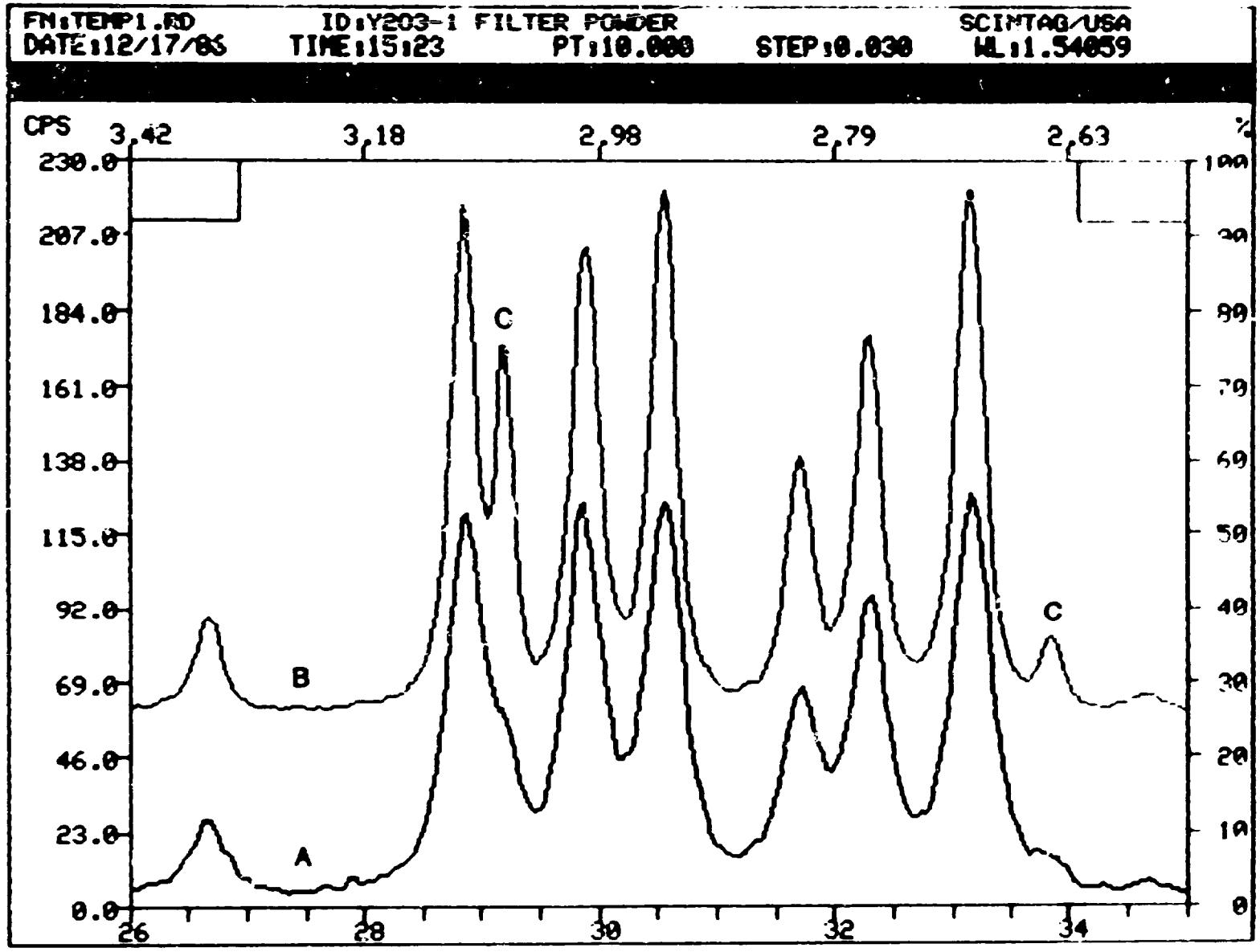
FN:TEMP1.RD
ID:Y203-1 FILTER POWDER
SCINTAG/USA
DATE:12/17/98
TIME:15:23
PT:10.000
STEP:0.030
WL:1.54059
CPS
3.42
3.18
2.98
2.79
2.63
%
230.0
207.0
184.0
161.0
138.0
115.0
92.0
69.0
46.0
23.0
0.0
100
90
80
70
60
50
40
30
20
10
0
A
B
C
C
26
28
30
32
34

Fig 4

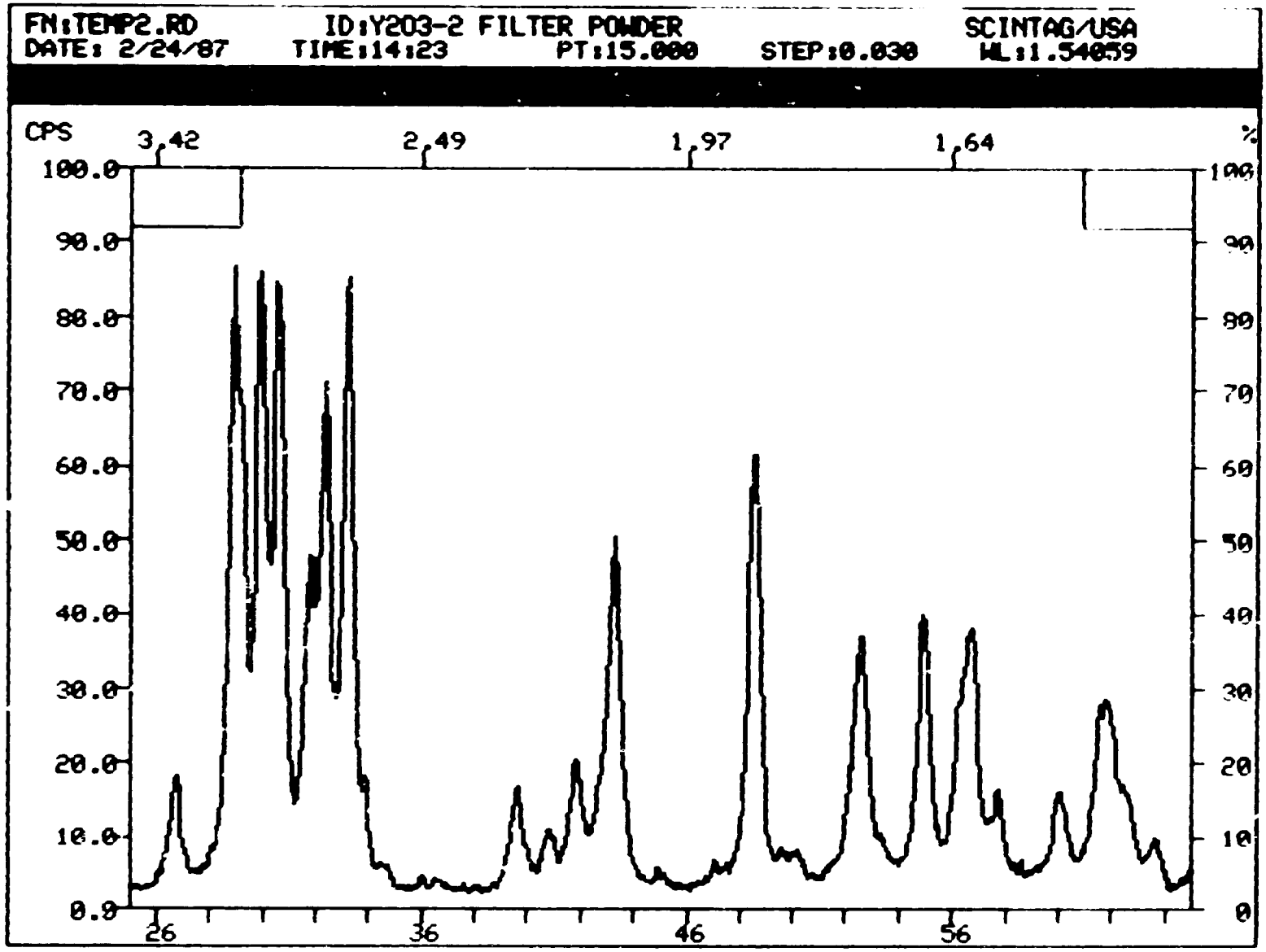
FN:TEMP2.RD
ID:Y203-2 FILTER POWDER
SCINTAG/USA
DATE: 2/24/87
TIME:14:23
PT:15.000
STEP:0.030
WL:1.54059
CPS
%
3.42
2.49
1.97
1.64
100.0
90.0
80.0
70.0
60.0
50.0
40.0
30.0
20.0
10.0
0.0
26
36
46
56